Published OnlineFirst June 13, 2011; DOI: 10.1158/0008-5472.CAN-11-0241

Tumor and Stem Cell Biology

Cancer Research

Microvesicles Released from Human Renal Cancer Stem Cells Stimulate Angiogenesis and Formation of Lung Premetastatic Niche

Cristina Grange[1], Marta Tapparo[1], Federica Collino[1], Loriana Vitillo[1], Christian Damasco[1], Maria Chiara Deregibus[1], Ciro Tetta[2], Benedetta Bussolati[1], and Giovanni Camussi[1]

Abstract

Recent studies suggest that tumor-derived microvesicles (MV) act as a vehicle for exchange of genetic information between tumor and stromal cells, engendering a favorable microenvironment for cancer development. Within the tumor mass, all cell types may contribute to MV shedding, but specific contributions to tumor progression have yet to be established. Here we report that a subset of tumor-initiating cells expressing the mesenchymal stem cell marker CD105 in human renal cell carcinoma releases MVs that trigger angiogenesis and promote the formation of a premetastatic niche. MVs derived only from CD105-positive cancer stem cells conferred an activated angiogenic phenotype to normal human endothelial cells, stimulating their growth and vessel formation after *in vivo* implantation in immunocompromised severe combined immunodeficient (SCID) mice. Furthermore, treating SCID mice with MVs shed from CD105-positive cells greatly enhanced lung metastases induced by i.v. injection of renal carcinoma cells. Molecular characterization of CD105-positive MVs defines a set of proangiogenic mRNAs and microRNAs implicated in tumor progression and metastases. Our results define a specific source of cancer stem cell–derived MVs that contribute to triggering the angiogenic switch and coordinating metastatic diffusion during tumor progression. *Cancer Res; 71(15); 5346–56. ©2011 AACR.*

Introduction

Recent studies showed that exosomes/microvesicles (MV) released by cells act as mediator of intercellular communications (1–3). Tumor cells produce large amount of MVs that may enter in the circulation and in other biological fluids (4, 5). It has been suggested that MVs, due to their pleiotropic effect, could be involved in cancer development, progression, and formation of the premetastatic niche (6). MVs contain mRNAs, microRNAs (miRNA), and proteins that could be transferred to target cells inducing epigenetic changes (7–10). Moreover, tumor-derived MVs may transport to neighboring cells, the products of oncogenes (11). Emerging evidence suggests that, in cancer patients, circulating miRNAs are stable in blood, probably due to their incorporation in exosomes/microvesicles, allowing their use as novel diagnostic markers (12).

Authors' Affiliations: [1]Department of Internal Medicine, Molecular Biotechnology Center and Center for Experimental Medicine (CeRMS), University of Torino, Turin, Italy; and [2]Fresenius Medical Care, Bad Homburg, Germany

Note: Supplementary data for this article are available at Cancer Research Online (http://clincancerres.aacrjournals.org/).

Corresponding Author: Giovanni Camussi, Dipartimento di Medicina Interna, Corso Dogliotti 14, 10126, Turin, Italy. Phone: 39-011-6336708; Fax: 39-011-6631184; E-mail: giovanni.camussi@unito.it

doi: 10.1158/0008-5472.CAN-11-0241

It is generally recognized that tumors contain a heterogeneous population of cells with different proliferation and differentiation potential. The majority of cells that form tumors are designated to differentiate and ultimately to stop dividing. At variance, a minor population of cells, defined as cancer stem cells or tumor-initiating cells, possess self-renewal capability and can induce tumors in immunocompromised animals (13). Recently, we identified in human renal cell carcinoma a subset of tumor-initiating cells expressing the mesenchymal stem cell marker CD105 that display stem cell properties, such as clonogenic ability, expression of Nestin, Nanog, and Oct3-4 stem cell markers, and lack of epithelial differentiation markers (14). This $CD105^+$ population has the capacity to generate epithelial and endothelial cells and serially transplantable tumors *in vivo* (14).

Previous studies showed that normal stem cells are an abundant source of MVs that may act as paracrine mediators by a horizontal transfer of genetic information (7, 8, 15).

The aim of the present study was to evaluate whether MVs released by $CD105^+$ cancer stem cells of renal carcinomas may modify tumor microenvironment by triggering angiogenesis and may favor the formation of a premetastatic niche.

Material and Methods

Cell culture

Human umbilical vein endothelial cells (HUVEC) were obtained and characterized as previously described (8). $CD105^+$ cancer stem cells, 3 deriving $CD105^+$ clones,

Published OnlineFirst June 13, 2011; DOI: 10.1158/0008-5472.CAN-11-0241

$CD105^-$ tumor cells, and unsorted tumor cells were previously isolated and characterized (14). Briefly, cell suspension obtained from 5 specimens of renal carcinomas of patients undergoing radical nephrectomy with informed consent were either used to generate unsorted tumor cells or sorted by anti-CD105 magnetic beads (MACS system; Miltenyi Biotec; ref. 14). To avoid the presence of nonneoplastic contaminating cells, $CD105^+$ cancer stem cells either were grown in expansion medium without serum (14) or were cloned. Three clones originating from 3 different renal cell carcinomas were used. The $CD105^-$ population could not generate clones. The $CD105^+$ clones and the total $CD105^+$ cell population were negative for the endothelial or hematopoietic markers CD31, VEGF receptor (VEGFR) 2, and CD45. In addition, they showed cancer stem cells properties as expression of stem cell markers and lack of differentiative markers, ability to grow in spheres, and the ability to initiate tumors and generate serially transplantable tumors with a number of cells as few as 100 cells per mouse (Supplementary Table S1). All cell types were thawed, used within 2 months, and the phenotype was characterized by fluorescence-activated cell-sorting (FACS) analysis and immunofluorescence immediately before the generation of MVs. The previously described (16) K1 renal tumor cell line was thawed and characterized by FACS immediately before their use for metastases generation.

Isolation and characterization of MVs

MVs were obtained from cell supernatants by ultracentrifugation as previously described (8). The protein content of MV preparations was quantified by Bradford method (Bio-Rad). In selected experiments, MVs were labeled with the red PKH26 dye (Sigma). The mean diameter of MVs and zeta potential were determined using a Malvern dynamic light-scattering spectrophotometer (Malvern Zetasizer 3000HS) and by transmission electron microscopy (17). Cytofluorimetric analysis was carried out as described (17), using the following fluorescein isothiocyanate (FITC)- or phycoerythrin (PE)-conjugated antibodies: CD44 (Dakocytomation), CD73, and CD29 (BD Biosciences), CD105, α5-integrin, α6-integrin, and HLA class I (BioLegend). FITC or PE mouse isotypic IgG (Dakocytomation) were used as controls. Beads of different sizes (1, 2, and 4 μm; Invitrogen) were used as size markers. In selected experiments, $CD105^+$ MVs derived from cloned $CD105^+$ cancer stem cells were treated with 1 U/mL RNase (Ambion) for 3 hours at 37°C (RNase $CD105^+$ MV; refs. 9, 10). After RNase treatment, the reaction was stopped by the addition of 10 U/mL RNase inhibitor (Ambion) and MVs were washed by ultracentrifugation. The efficacy of RNase treatment was evaluated by MV RNA analyses by Agilent 2100 bioanalyzer (Agilent Technologies) and by 0.6% agarose gel electrophoresis.

mRNA analysis

RNA from MVs was isolated using the RNAqueous Micro Kit (Ambion). RNA was quantified spectrophotometrically (Nanodrop ND-1000), and its quality was assessed by Agilent 2100 Bioanalyzer. mRNA expression levels were analyzed using the RT^2 Profiler PCR array system (SABiosciences-Qiagen) to profile 84 genes involved in angiogenesis by real-time (RT-PCR). A pool of RNA from 4 MV preparations (400 ng $CD105^+$ or $CD105^-$ MVs) was retrotranscribed and run on 7900HT RT-PCR instrument (Applied Biosystems). Raw C_t values were calculated using SDS software (version 2.3), using automatic baseline and threshold. Quantitative RT-PCR (qRT-PCR) validation of gene array data was carried out using SYBR green technique (Supplementary Material).

miRNA analysis

RNA was isolated using the *mirVana* miRNA Isolation Kit (Ambion). TaqMan MicroRNA Assay Human Panel Early Access kit (Applied Biosystems) was employed to profile 365 mature miRNAs by qRT-PCR. Sixty nanograms of RNA from $CD105^+$ or $CD105^-$ MVs was analyzed. Raw C_t values were calculated using the SDS software. miRNAs with raw C_t values greater than 35 in both preparations were not included in the analysis, as they were considered nonspecific (18, 19). Using filtering criteria, 82 and 87 miRNAs present in $CD105^+$ and $CD105^-$ MVs, respectively, were included in the analysis. As the small nucleolar RNAs (snoRNAs; internal controls) were undetectable in MV preparations, endogenous control was calculated using the mean value of 4 of the most stable miRNAs between $CD105^+$ MVs and $CD105^-$ MVs (hsa-miR-181b, -27a, -484, and -324-3p; refs. 20, 21). Relative quantification (RQ) was obtained using the equation $2^{(-\Delta\Delta C_t)}$ (where $\Delta\Delta C_t$ is the difference between ΔC_t $CD105^+$ MVs and ΔC_t $CD105^-$ MVs; ΔC_t = mean C_t miRNA − mean C_t of endogenous control). To confirm some miRNAs identified by microarray analysis, qRT-PCR, using SYBR green technique, was carried out (Supplementary Material).

Gene targets analysis

The software TargetScan (http://www.targetscan.org) was employed to predict genes target for upregulated miRNAs in $CD105^+$ MVs. To define a core list, genes that were target of at least 5 miRNAs were selected. This group of genes was searched for GO (Gene Ontology) term enrichment, using the GO annotations (http://www.geneontology.org). We used Fisher's exact test to evaluate GO keywords overrepresentation. A P value of more than 10^{-4} was considered as statistically significant for GO terms overrepresentation.

Internalization of MVs

HUVEC labeled with carboxyfluoroscein succinimidyl ester (CSFE Vybrant CFDA SE Cell Tracer Kit; Molecular Probe) were incubated for 1 hour at 37°C with PKH26-labeled $CD105^+$ and $CD105^-$ MVs, and after washing they were analyzed by confocal microscopy (LSM 5 Pascal; Carl Zeiss International; ref. 17). Hoechst 33258 dye (Sigma) was added for nuclear staining.

In vitro angiogenesis assay

In vitro formation of capillary-like structures was done on growth factor–reduced Matrigel (BD Biosciences; ref. 8). HUVECs (3×10^4 cells per well) were seeded onto Matrigel-coated wells in RPMI + 5% fetal calf serum (FCS) with or without 30 μg/mL MVs. Cell organization onto Matrigel was

Published OnlineFirst June 13, 2011; DOI: 10.1158/0008-5472.CAN-11-0241

microscopically recorded after 16 hours. Data were expressed as the mean ± SD of tubule length in arbitrary units per field.

Invasion, apoptosis, and adhesion assays

The effect of CD105$^+$ MVs, RNase CD105$^+$ MVs, CD105$^-$ MVs, and unsorted tumor MVs on Matrigel invasion and apoptosis resistance of HUVECs and on adhesion of K1 tumor cells to HUVEC were evaluated. Invasion was evaluated in 24-well cell culture inserts (BD Biosciences) with a porous membrane (8.0-μm pore size) precoated with 100 μg Matrigel per well as described (21). Total area of invaded Matrigel (magnification × 100) was evaluated by MicroImage analysis system (Cast Imaging srl). Apoptosis was carried out using terminal deoxynucleotidyl transferase–mediated dUTP nick end labeling (TUNEL) assay (ApopTag Fluorescein Direct In Situ Apoptosis; Millipore). Adhesion assay was carried out on HUVEC monolayer pretreated for 24 hours at 37°C in RPMI + 5% FCS with or without MVs. Renal K1 tumor cells (5×10^5 per well), labeled with CSFE, were added to the endothelial monolayer. The adhesion assay in static conditions was evaluated after 6 hours. After washings, cells adherent to HUVECs were counted by fluorescence microscopy (magnification × 200) in 10 fields and expressed as mean ± SD of cells per field.

In vivo angiogenesis

Animal experiments were carried out according to the guidelines for the care and use of research animals and

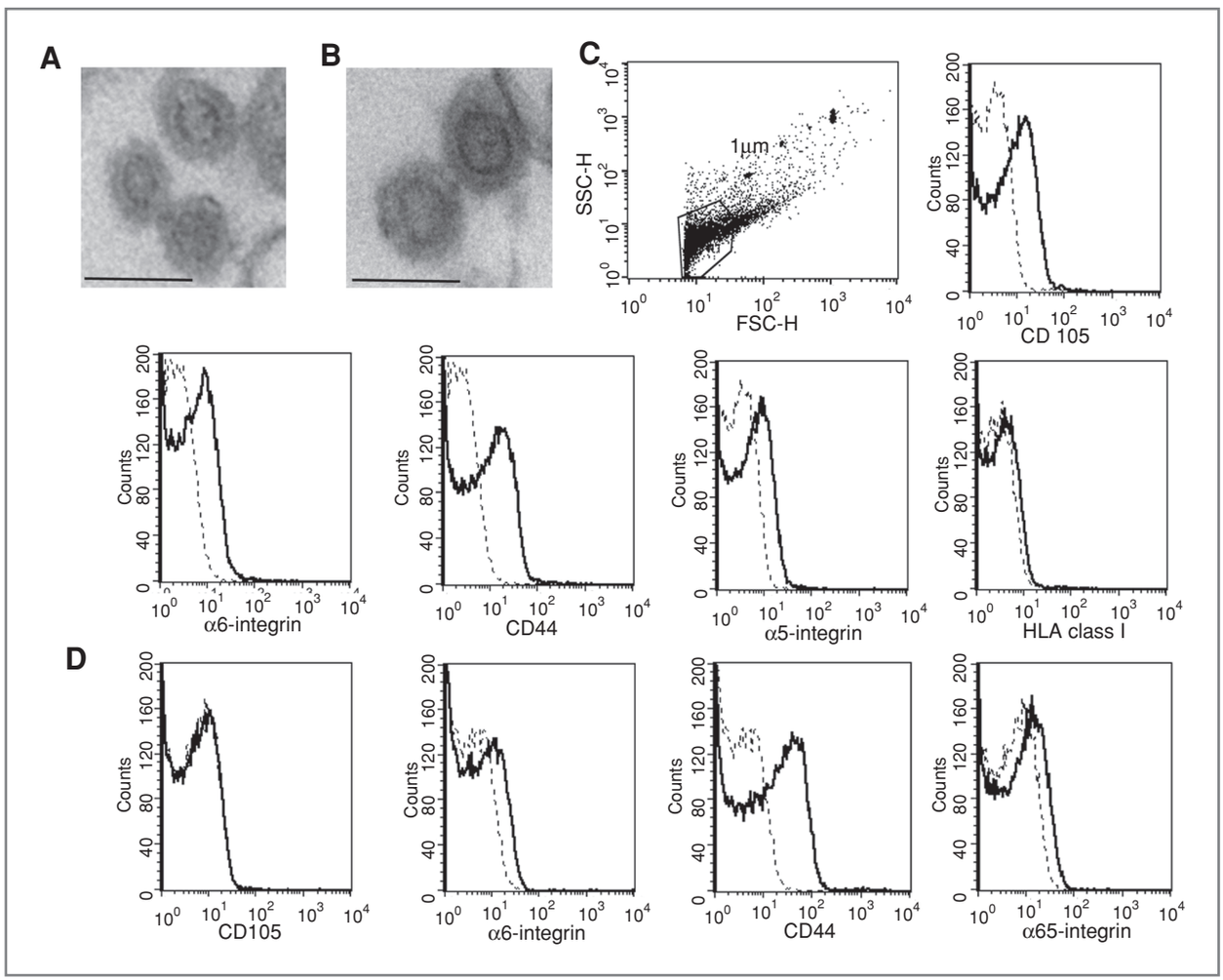

Figure 1. Characterization of MVs. Representative micrographs of transmission electron microscopy of CD105$^+$ MVs (A) and CD105$^-$ MVs (B) showing a spheroid shape (original magnification ×10,000; bar, 100 nm). CD105$^-$ MVs display the same morphology and size (not shown). C, representative FACS analyses of CD105$^+$ MVs showing the size (with 1, 2, and 4-μm beads used as internal size standards) and the expression of CD105, α6-integrin, CD44, α5-integrin, and HLA class I (thick lines) surface molecules. In the CD105, α6-integrin, CD44, and α5-integrin experiments, the Kolmogrov–Smirnov statistical analysis between relevant antibodies and the isotypic control was significant ($P < 0.001$). No significant expression of HLA class I was observed. D, representative cytofluorimetric analyses of CD105$^-$ MVs showing the expression of α6-integrin, CD44, α5-integrin (the Kolmogrov–Smirnov statistical analysis between relevant antibodies and the isotypic control was significant: $P < 0.001$). CD105 was negative. Dotted lines indicate the isotopic controls. MV preparations derived from 3 CD105$^+$ clones, 5 CD105$^+$ uncloned cancer stem cells, and 5 CD105$^-$ tumor cells were analyzed with similar results.

Published OnlineFirst June 13, 2011; DOI: 10.1158/0008-5472.CAN-11-0241

were approved by the local Ethics Committee. HUVEC, prestimulated with or without 70 μg MVs, were implanted subcutaneously into severe combined immunodeficient (SCID) mice (Charles River) within Matrigel (22). At day 10, mice were sacrificed and the Matrigel plug was recovered. Angiogenesis was calculated as the mean ± SD of the number of vessels with red cells inside per total area of hematoxylin and eosin–stained sections. Immunohistochemistry was carried out using anti-HLA class I (Santa Cruz Biotechnology) and anti-von Willebrand factor (vWF; Dakocytomation) antibody.

In vivo metastasis

SCID mice were injected intravenously daily for 5 days with 70 μg of MVs in 100 μL PBS. On day 5, mice received an i.v. injection into the tail vein of 6×10^5 renal K1 tumor cells. Mice were sacrificed after 5 weeks, and organs (lung, spleen, liver, and kidney) were collected for histology. Lung metastases were counted in 5 nonsequential serial sections; results were expressed as mean ± SD of metastasis per lung (23). On day 5, a total of 8 mice treated with $CD105^+$ MVs, $CD105^-$ MVs, and PBS (vehicle) were sacrificed and their lungs processed for histology, RNA extraction, and murine endothelial cells sorting using magnetic beads anti-CD146 (MACS system; Supplementary Fig. S1 and Supplementary Material). Immunohistochemistry was carried out using matrix metalloproteinases (MMP) anti-MMP2 and MMP9 (Santa Cruz Biotechnology) antibodies. Cytofluorimetric analysis on lung endothelial cells was carried out using anti-CD31, anti-CD146 (BD Biosciences), anti-CD45 (Miltenyi), anti-VEGFR1 (R&D), and anti-α6-integrin (Biolegend) monoclonal antibodies. qRT-PCR for murine MMP9, MMP2, and VEGF was carried out using SYBR green technique on total lung tissues and endothelial cell fractions (Supplementary Material).

Statistical methods

Differences were determined by Student's t test or by ANOVA followed by the Newman–Keuls multicomparison test when appropriate. A value of $P < 0.05$ was considered significant.

Results

Characterization of MVs shed by $CD105^+$ renal cancer stem cells

MVs released from $CD105^+$ cancer stem cells ($n = 5$) and deriving clones ($n = 3$) were compared with MVs released from $CD105^-$ tumor cells ($n = 5$). MVs generated by $CD105^+$ cancer stem cells and derived clones and by the $CD105^-$ tumor cells had the same morphology and size, ranging from 10 to 100 nm as determined by zeta-size analysis and electron microscopy (Fig. 1A and B). Moreover, they showed the same zeta potential of -22.4 ± 3.5 mV. By cytofluorimetric analysis, MVs were detected below the forward scatter signal corresponding to 1-μm beads. The main difference between MVs

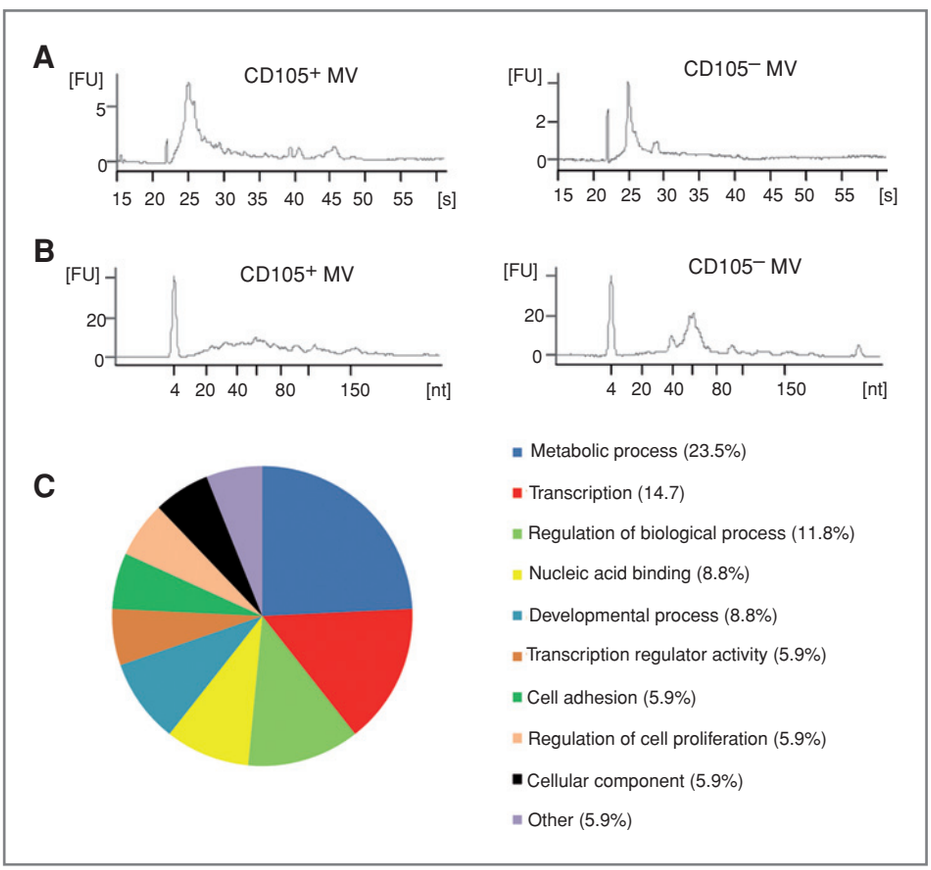

Figure 2. Characterization of MV RNAs. A, representative bioanalyzer profile of the RNAs contained in $CD105^+$ MVs derived from $CD105^+$ clones and in $CD105^-$ MVs showing that the ribosomal subunits 28S and 18S were absent or barely detectable. B, representative bioanalyzer profile of small RNAs was obtained using RNA subtypes present in $CD105^+$ MVs and $CD105^-$. Three different samples tested in triplicate were analyzed with similar results. C, GO enrichment analysis of target genes of at least 5 upregulated miRNAs in $CD105^+$ MVs. Fisher's exact test to evaluate GO keywords overrepresentation was used. A $P < 10^{-4}$ was considered statistically significant for GO terms. Overrepresented biological processes are grouped according to their common ancestor.

Published OnlineFirst June 13, 2011; DOI: 10.1158/0008-5472.CAN-11-0241

derived from CD105$^+$ cancer stem cells and CD105$^-$ tumor cells was the expression of CD105 present only on MVs derived from CD105$^+$ cells (CD105$^+$ MVs) but not on those derived from CD105$^-$ cells (CD105$^-$ MVs). Both CD105$^+$ and CD105$^-$ MVs expressed CD44 and adhesion molecules such as α5- and α6-integrins (Fig. 1C and D) as the cells of origins, whereas CD29 was barely detectable in CD105$^+$ MVs and negative in CD105$^-$ MVs (not shown). Both MV types did not express HLA class I (Fig. 1) and CD73 (not shown).

Characterization of RNAs shuttled by MVs

We carried out a bioanalyzer profile of total RNA present in CD105$^+$ MVs from cloned cancer stem cell preparations and CD105$^-$ MVs. Both MVs contained RNA of different size, suggesting the presence of mRNAs and of small RNAs compatible with the presence of miRNAs, whereas the ribosomal subunit 28S and 18S were barely detectable (Fig. 2A). In the CD105$^+$ MVs, we observed an enrichment of small RNAs of the size of miRNAs (42.3% ± 2.5%) in comparison with CD105$^-$ MVs (20.2% ± 1.7%; Fig. 2B). miRNA expression by MVs shed from CD105$^+$ and CD105$^-$ cells was then screened by qRT-PCR profiling 365 human mature miRNAs. CD105$^+$ and CD105$^-$ MVs revealed the presence of 82 and 87 miRNAs, respectively. Twenty-four miRNAs were significantly upregulated in CD105$^+$ MVs with respect to CD105$^-$ MVs, whereas 33 miRNAs were significantly downregulated (Table 1). To confirm data obtained from miRNA screening, single miRNAs were selected and analyzed in 3 different preparations of CD105$^+$ and CD105$^-$ MVs by qRT-PCR (Supplementary Table S2). To characterize the biological processes modulated by the upregulated miRNAs present in CD105$^+$ MVs, we analyzed their target genes predicted by TargetScan algorithm, selecting those genes targeted by almost 5 miRNAs. This list counted 157 genes (Supplementary Table S3). We carried out the functional characterization of the gene target list searching for GO keywords enrichment and we found a strong overrepresentation of terms belonging to crucial biological processes such as transcription, metabolic process, nucleic acid binding, cell adhesion molecules, and regulation of cell proliferation (Fig. 2C and Supplementary Table S4).

Moreover, we investigated whether CD105$^+$ MVs contained mRNAs involved in the stimulation of angiogenesis in comparison with CD105$^-$ MVs. mRNAs of genes involved in angiogenesis were detected only in CD105$^+$ MVs. In particular, they contained mRNAs for growth factors such as VEGF, fibroblast growth factors 2 (FGF2), angiopoietin1, and ephrin A3 and for MMP2 and MMP9. Each mRNA detected was confirmed on 3 different CD105$^+$ MV preparations by using qRT-PCR.

In vitro activation of HUVEC by CD105$^+$ MVs

To evaluate whether MVs derived from CD105$^+$ renal cancer stem cells could be responsible for stimulating tumor angiogenesis and invasion, we compared their effects with MVs from CD105$^-$ tumor cells. We first evaluated the uptake of CD105$^+$ and CD105$^-$ MVs labeled with PKH26 dye by HUVEC, after 1-hour incubation at 37°C. HUVECs incorporated in equal manner both CD105$^+$ and CD105$^-$ MVs (Fig. 3A).

Table 1. miRNAs differentially expressed in CD105$^+$ MVs with respect to CD105$^-$ MVs

Downregulated		Upregulated	
miRNA	**RQ**	**miRNA**	**RQ**
hsa-miR-142-5p	0.0006	hsa-miR-200c	133.9685
RNU6B	0.0040	hsa-miR-146a	68.6291
hsa-miR-15a	0.0162	hsa-miR-184	34.3860
hsa-miR-129	0.01657	hsa-miR-335	34.2195
hsa-miR-101	0.0396	hsa-miR-646	30.2686
hsa-miR-296	0.0651	hsa-miR-449b	19.5724
hsa-miR-145	0.0694	hsa-miR-650	12.9308
hsa-miR-361	0.0874	hsa-miR-141	9.2135
hsa-miR-23b	0.1088	hsa-miR-183	7.3653
hsa-miR-23a	0.1385	hsa-miR-19b	4.2390
hsa-miR-100	0.1470	hsa-miR-29c	3.4791
hsa-miR-99b	0.1985	hsa-miR-182	3.1749
hsa-miR-324-5p	0.2096	hsa-miR-19a	3.1010
hsa-miR-30a-5p	0.2379	hsa-miR-92	3.0903
hsa-let-7b	0.2441	hsa-miR-301	2.8064
hsa-miR-7	0.2555	hsa-miR-151	2.7697
hsa-miR-15b	0.2622	hsa-miR-130b	2.6884
hsa-miR-27b	0.2986	hsa-miR-29a	2.3097
hsa-let-7f	0.3062	hsa-miR-22	2.1927
hsa-miR-615	0.3205	hsa-miR-186	2.1565
hsa-miR-218	0.3264	hsa-let-7g	2.1313
hsa-miR-328	0.3407	hsa-miR-140	2.1239
hsa-miR-10a	0.3594	hsa-miR-486	2.1210
hsa-miR-222	0.3697	hsa-miR-26b	2.0601
hsa-let-7a	0.3741		
hsa-miR-342	0.3881		
hsa-miR-125a	0.3922		
hsa-miR-572	0.3965		
hsa-miR-149	0.4018		
hsa-miR-30d	0.4114		
hsa-let-7c	0.4418		
hsa-miR-451	0.4593		
hsa-miR-25	0.4798		

NOTE: RQ was obtained using the equation $2^{(-\Delta\Delta C_t)}$ (where $\Delta\Delta C_t$ is the difference between ΔC_t CD105$^+$ MVs and ΔC_t CD105$^-$ MVs; ΔC_t = mean C_t miRNA − mean C_t of endogenous control).

CD105$^+$ MVs from cancer stem cells and deriving clones stimulated HUVEC to organize *in vitro* into capillary-like structures on Matrigel. In contrast, CD105$^-$ MVs did not induce the formation of capillary-like structures. MVs derived from unsorted tumor cells also induced the formation of capillary-like structures, but the proangiogenetic effect of MVs from CD105$^+$ sorted cells was significantly greater (Fig. 3B and C). Moreover, CD105$^+$ MVs, but not CD105$^-$ MVs, significantly enhanced the invasion of HUVECs through Transwells coated with Matrigel, with respect to CD105$^-$ MVs as well as to MVs from unsorted tumor cells (Fig. 4A and B). CD105$^+$ MVs also

Published OnlineFirst June 13, 2011; DOI: 10.1158/0008-5472.CAN-11-0241

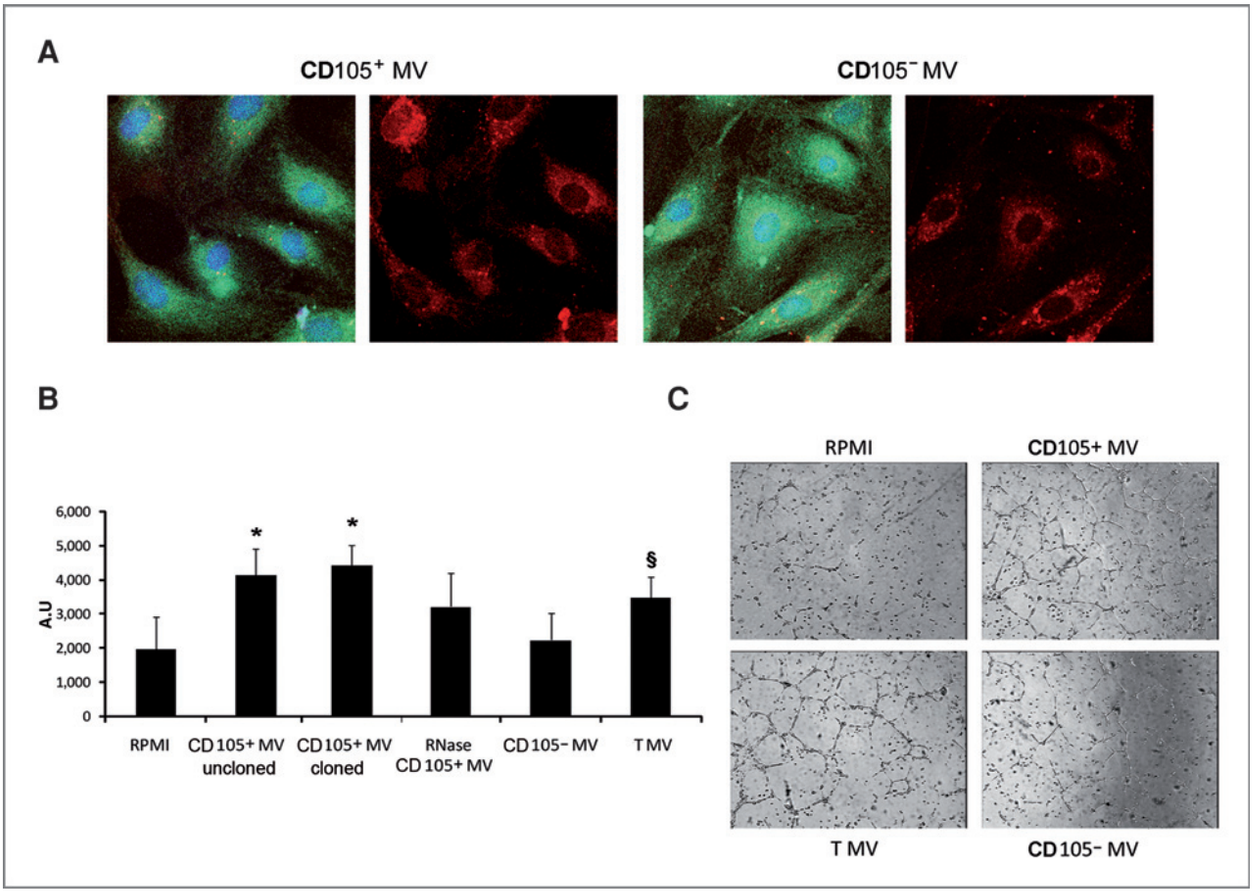

Figure 3. Internalization of MVs in HUVECs and *in vitro* angiogenic effect. A, representative confocal microscopy analysis of red-labeled MVs in HUVECs stained with CFSE (green). Seven experiments were carried out with similar results (original magnification ×630). Quantitative evaluation (B) and representative micrographs (C) showing the formation of capillary-like structure formed by HUVECs seeded on Matrigel-coated plates in a serum-starved condition (RPMI) and stimulated with 30 μg/mL of $CD105^+$ MVs from uncloned and cloned cancer stem cell preparations, RNase $CD105^+$ MVs derived from cloned cancer stem cells, $CD105^-$ MVs, and MVs from unsorted tumor cell (TMV). Data are expressed as the mean ± SD of the length of capillary-like structure after 16 hours, evaluated by the computer analysis system in arbitrary units (AU) in at least 10 different fields at ×200 magnification. Four different experiments per group were carried out in duplicate. ANOVA with the Newman–Keuls multicomparison test was carried out: *, $P < 0.05$, $CD105^+$ MV versus RPMI, RNase $CD105^+$ MV, $CD105^-$ MV, and TMV; §, $P < 0.05$, TMV versus RPMI and $CD105^-$ MV.

induced a greater apoptosis resistance in HUVECs treated with 100 ng/mL of doxorubicin (Fig. 4C). To investigate whether MV treatment could modify the adhesive property of endothelial cells, HUVECs were pretreated with different MVs and, after 6 hours, the adhesion of renal tumor cells was evaluated. $CD105^+$ MVs significantly enhanced the adhesion of tumor cells with respect to $CD105^-$ MVs and unsorted tumor MVs (Fig. 4D). MVs from unsorted tumor cells induced invasion, apoptosis resistance, and tumor cells adhesion in HUVECs that were greater with respect to $CD105^-$ MVs or vehicle, suggesting that the effects observed by tumor cell–derived MVs should be ascribed to MVs released from cancer stem cells.

RNase pretreatment of $CD105^+$ MVs significantly reduced *in vitro* capillary-like formation (Fig. 3B), as well as the enhanced invasion, apoptosis resistance, and adhesion properties (Fig. 4), suggesting a role of RNA molecular species carried by MVs.

In vivo effects of $CD105^+$ MVs

To evaluate whether $CD105^+$ MVs were able to stimulate angiogenesis *in vivo*, we subcutaneously injected MV-stimulated HUVECs within Matrigel in SCID mice. $CD105^+$ MVs from cloned cancer stem cell preparations stimulated the growth of HUVECs that formed dense clusters containing small vessels organized into patent capillaries connected with the murine vasculature and into large aneurismatic structures (Fig. 5A). The cells grew into Matrigel, and the vessels expressed the endothelial marker vWF and their human nature was shown by staining for HLA class I (Fig. 5B). HUVECs challenged with vehicle or $CD105^-$ MVs or RNase $CD105^+$ MVs did not organize or proliferate into the Matrigel. MVs from unsorted tumor cells induced HUVEC proliferation and organization into small vessels, but the extent of angiogenesis was significantly lower than that induced by $CD105^+$ MVs (Fig. 5C).

To evaluate whether $CD105^+$ MVs contribute to establish a premetastatic niche, we intravenously injected SCID mice for

Published OnlineFirst June 13, 2011; DOI: 10.1158/0008-5472.CAN-11-0241

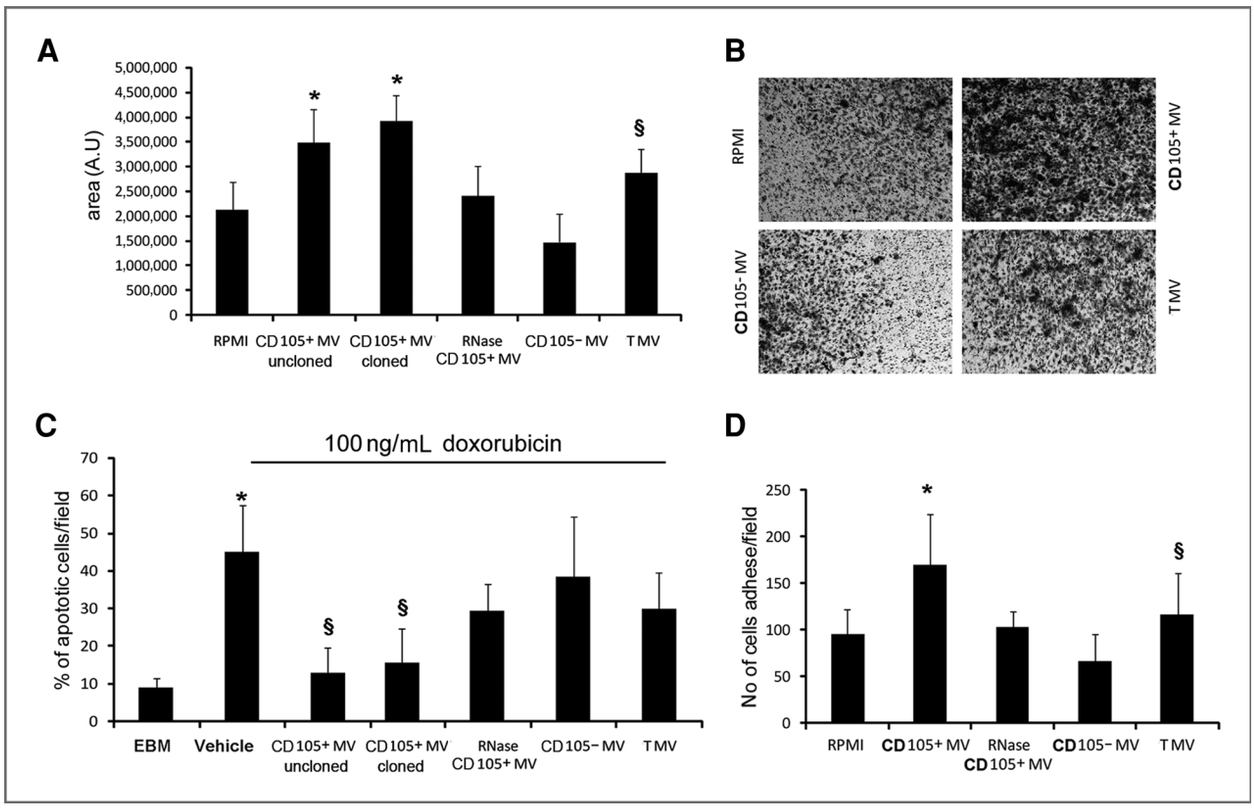

Figure 4. Effect of MVs on endothelial cell invasion, apoptosis resistance, and tumor cell adhesion to endothelium. Quantitative evaluation (A) and representative micrographs (B) showing the invasion of Matrigel-coated Transwells by HUVECs stimulated with 30 μg/mL of MVs from uncloned and cloned cancer stem cell preparations, RNase $CD105^+$ MVs, $CD105^-$ MVs, and TMVs. Invasion was evaluated after 24 hours. Data are expressed as the mean ± SD of the area occupied by cells on total well-surface area evaluated by the computer analysis system in arbitrary units (AU) at ×100 magnification. ANOVA with the Newman–Keuls multicomparison test was carried out: *, $P < 0.05$, $CD105^+$ MV versus RPMI, RNase $CD105^+$ MV, $CD105^-$ MV, and TMV; §, $P < 0.05$: TMV versus RPMI and $CD105^-$ MV. C, quantitative evaluation of apoptosis of HUVECs cultured in the presence of 100 ng/mL of doxorubicin plus vehicle or 30 μg/mL of MVs from uncloned and cloned cancer stem cell preparations, RNase $CD105^+$ MVs, $CD105^-$ MVs, and TMVs. Apoptosis was evaluated by TUNEL assay after 24 hours as percentage (mean ± SD of cells per field) of apoptotic cells per field. As control, cells were cultured in endothelial basal medium (EBM) in the absence of doxorubicin. ANOVA with the Newman–Keuls multicomparison test was carried out: *, $P < 0.05$, doxorubicin treatment in the presence of vehicle alone, RNase $CD105^+$ MV, $CD105^-$ MV, and TMV induced significant apoptosis versus doxorubicin untreated (EBM); §, $P < 0.05$: $CD105^+$ MV significantly inhibited apoptosis versus all other doxorubicin treatment (vehicle, RNase $CD105^+$ MV, $CD105^-$ MV, and TMV). D, quantitative evaluation (mean ± SD of cells per field) of adhesion of 5×10^5 K1 tumor cells labeled with CSFE to a monolayer of HUVEC unstimulated (RPMI) or stimulated with 30 μg/mL of MVs from cloned cancer stem cell preparations, RNase $CD105^+$ MVs, $CD105^-$ MVs, and TMVs. ANOVA with the Newman–Keuls multicomparison test was carried out: *, $P < 0.05$, $CD105^+$ MV versus RPMI, RNase $CD105^+$ MV, $CD105^-$ MV, and TMV; §, $P < 0.05$ TMV versus RPMI and $CD105^-$ MV. For all the experimental condition, 5 different experiments were carried out in duplicate.

5 days with 70 μg of MVs, followed by i.v. injection of 6×10^5 renal tumor cells. After 5 weeks, organs were recovered (liver, spleen, kidney, and lung) and the incidence of metastasis was evaluated. Metastases clearly detectable were found only in lungs (Fig. 6A). The number of metastases induced by renal tumor cells was very low in mice injected with vehicle alone or with $CD105^-$ MVs or RNase $CD105^+$ MVs, whereas a significant increase in the number of metastases was observed in mice pretreated with $CD105^+$ MVs or MVs from unsorted tumor cells. However, $CD105^+$ MVs were significantly more efficient in inducing metastasis than unsorted tumor MVs (Fig. 6A). To evaluate whether the administration of MVs modify lung microenvironment, the expression of VEGFR1, VEGF, MMP9, and MMP2 was studied. By cytofluorimetric analysis, VEGFR1 expression in $CD146^+$-sorted lung endothelial cells was enhanced by $CD105^+$ MVs but not by $CD105^-$ MVs (Fig. 6B). By qRT-PCR, $CD105^+$ MVs, but not $CD105^-$ MVs, significantly enhanced MMP9 expression in total lung tissue and VEGF and MMP2 in sorted lung endothelial cells (Fig. 6C). The enhanced expression of MMP9 and MMP2 in lung after treatment with $CD105^+$ MVs was confirmed by immunohistochemistry (Fig. 6D). MMP2 staining was mainly confined to lung vessels, whereas that of MMP9 was more diffuse and the alveolar epithelial cells were positive.

Discussion

Previous studies showed an angiogenic potential of MVs derived from tumors but did not characterize the cells of origin (11, 24–26). Herein, we showed that in renal cancer, the MVs that retain the angiogenic properties were those that were derived from cancer stem cells. Indeed, MVs released

Published OnlineFirst June 13, 2011; DOI: 10.1158/0008-5472.CAN-11-0241

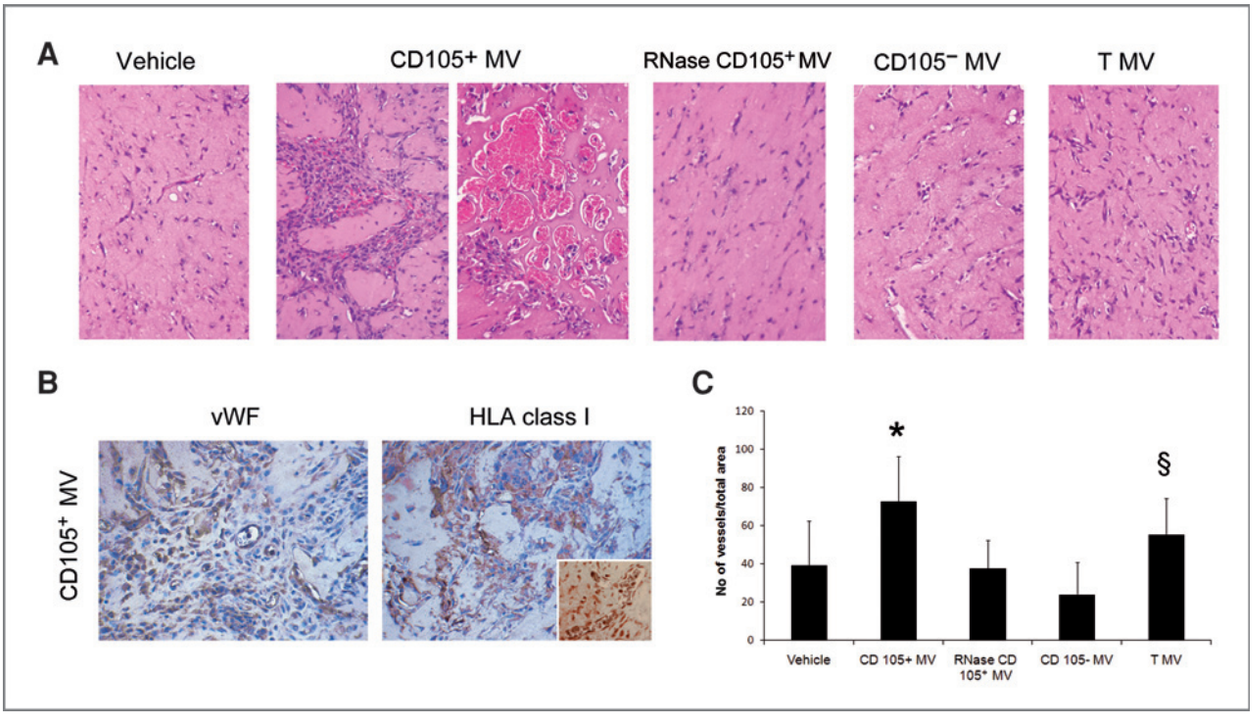

Figure 5. *In vivo* angiogenesis of HUVECs stimulated with $CD105^+$ MVs. HUVECs (1×10^6) treated with vehicle or 70 μg of $CD105^+$ MVs from cloned cancer stem cell preparations, RNase $CD105^+$ MVs, $CD105^-$ MVs, and TMVs were injected subcutaneously within Matrigel in SCID mice, and mice were sacrificed 10 days after. A, representative micrographs of hematoxylin and eosin staining of section of Matrigel showing dense cluster of cells infiltrated by small vessels and microaneurismatic structures containing erythrocytes in HUVECs stimulated with $CD105^+$ MVs. TMVs induced only the formation of small vessels. B, representative micrograph of immunostaining for the endothelial antigen (vWF) and for HLA class I antigen (original magnification ×200). C, quantitative evaluation of neo-formed vessels was expressed as the number of vessels per total area of Matrigel. Data are expressed as mean ± SD of 8 individual experiments for each condition. ANOVA with the Newman–Keuls multicomparison test was carried out: *, $P < 0.05$, $CD105^+$ MV versus vehicle, RNase $CD105^+$ MV, $CD105^-$ MV, and TMV; §, $P < 0.05$, TMV versus vehicle, RNase $CD105^+$ MV, and $CD105^-$ MV.

from cancer stem cells induced *in vitro* and *in vivo* angiogenesis and favored lung metastasis. These properties were ascribed only to the MVs released from the $CD105^+$ cell fraction, as those derived from the $CD105^-$ tumor cells were ineffective. Indeed, $CD105^+$ MVs contained proangiogenic mRNAs and miRNAs that may be involved in tumor progression and metastases.

Recently, circulating MVs were described in patients with various tumors (27–32), suggesting that they may serve as a diagnostic and prognostic tool (33–35). In the context of cancer, several studies pointed out the potential role of tumor-derived MVs in the interaction with stromal cells and in the formation of premetastatic niche (36–39). The potential of MVs to reprogram recipient cells was first established by Ratajczak and colleagues (7). Several subsequent studies indicate that mRNA delivered by MVs can be translated into the corresponding proteins by target cells (8, 9, 40).

In the present study, we investigated whether MVs derived from cancer stem cells possess biological activities that may account for the induction of a favorable environment for tumor growth and invasion. We found that MVs derived from $CD105^+$ renal cancer stem cells differ for their content of mRNAs and miRNAs with respect to the $CD105^-$ renal cancer cell population. In particular, $CD105^+$ MVs contained several proangiogenic mRNAs such as VEGF, FGF, angiopoietin1, ephrin A3, MMP2, and MMP9 that were absent in $CD105^-$ tumor MVs. The presence of the proangiogenic mRNAs correlated with an *in vitro* and *in vivo* angiogenic effect of $CD105^+$ MVs. The proangiogenic effect of $CD105^+$ MVs can be ascribed to their ability to induce endothelial cell growth, organization, invasion of matrix, and resistance to apoptosis. An angiogenic effect of MVs was previously described for MVs derived from unfractionated tumor cells of lung cancer, ovarian cancer, and glioblastoma, as well as from some tumor cell lines (11, 25, 26, 33). Beside mRNAs, MVs were shown to contain and to deliver functional miRNAs to target cells (9, 20). $CD105^+$ MVs were enriched in miRNAs with respect to the $CD105^-$ MVs. The GO analysis of predicted target genes indicated that $CD105^+$ MVs shuttled a selected pattern of miRNAs that may modulate several biological functions relevant for cell growth, regulation of transcription, cell matrix adhesion, and synthesis of macromolecules. Among the miRNAs shuttled by $CD105^+$ MVs, we detected miR-200c, miR-92, and miR-141 that were described significantly upregulated in patients with ovarian (28, 41), colorectal (42), and prostate cancer (43), respectively. These miRNAs were suggested as marker of unfavorable prognosis (44). In addition, we detected several miRNAs such as miR-29a, miR-650, and miR-151 that were associated with tumor invasion and metastases (45–47).

Published OnlineFirst June 13, 2011; DOI: 10.1158/0008-5472.CAN-11-0241

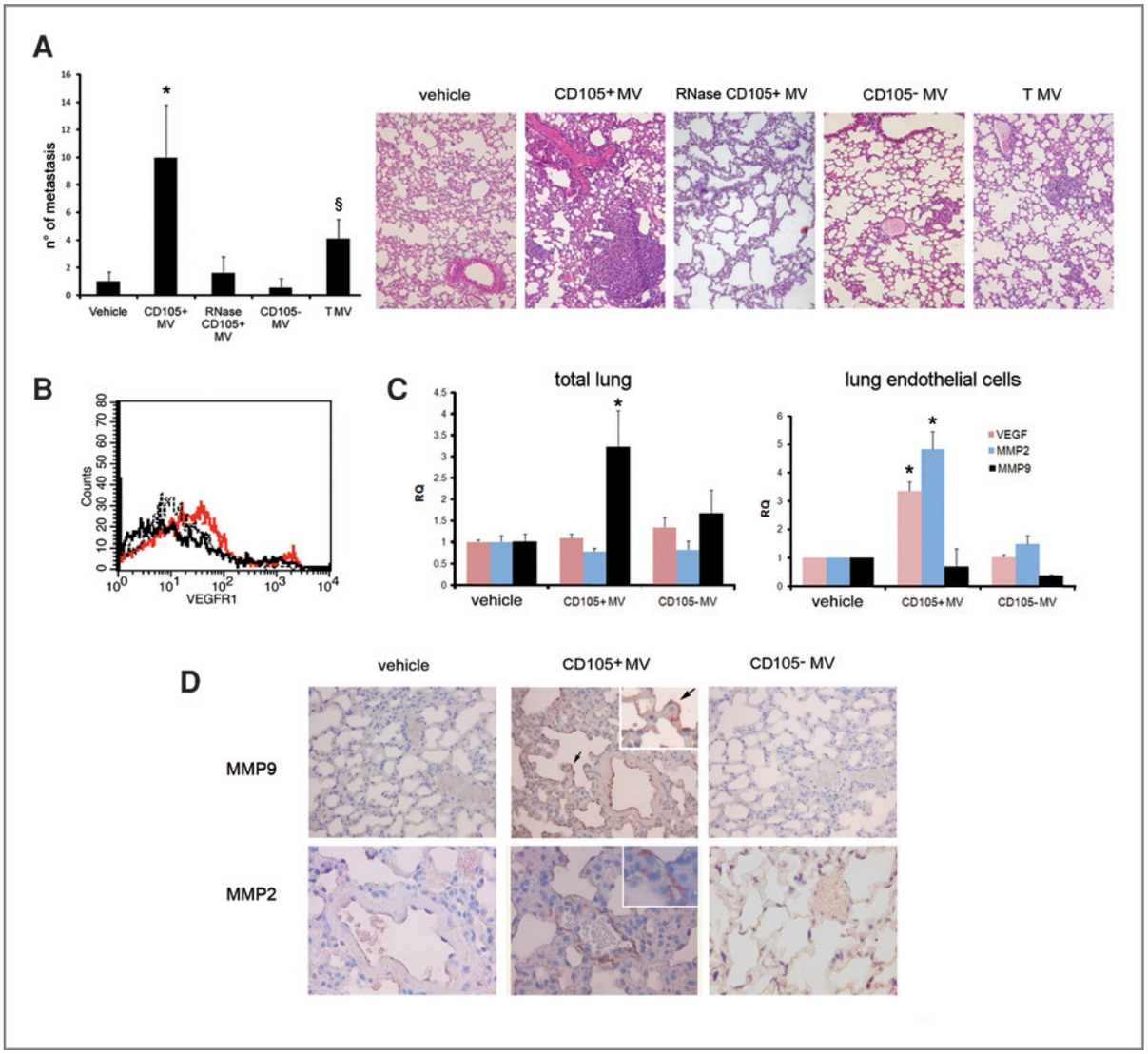

Figure 6. Effect of MVs on lung metastasis formation. SCID mice (5 per group) were treated for 5 days with i.v. injections of vehicle or 70 μg of $CD105^+$ MVs from cloned cancer stem cell preparations, RNase $CD105^+$ MVs, $CD105^-$ MVs, or TMVs. K1 renal tumor cells (6×10^5) were injected intravenously on day 5, and mice were sacrificed 5 weeks later. A, quantitative evaluation of metastases carried out in 5 nonconsecutive sections of whole lungs and expressed as mean ± SD per lung and representative hematoxylin and eosin–stained lung sections (original magnification ×200). ANOVA with the Newman–Keuls multicomparison test was carried out, *, $P < 0.05$, $CD105^+$ MV versus vehicle, RNase $CD105^+$ MV, $CD105^-$ MV, and TMV; §, $P < 0.05$, TMV versus vehicle, RNase $CD105^+$ MV, and $CD105^-$ MV. B, representative cytofluorimetric analysis of VEGFR1 expression by $CD146^+$-sorted lung endothelial cells obtained from mice treated for 5 days with 70 μg of $CD105^+$ MVs (red line) or $CD105^-$ MVs (dark line) or with vehicle alone (dotted line). The percentage of positive cells was as follows: $CD105^+$ MVs, 63% ± 3.1%; $CD105^-$ MVs, 36% ± 2.7%; vehicle, 40% ± 2.9%. Eight mice per group were studied with similar results. C, qRT-PCR analysis of VEGF, MMP2, and MMP9 mRNA expression in total lung and in $CD146^+$ endothelial cells of mice treated for 5 days with 70 μg of $CD105^+$ MVs or $CD105^-$ MVs or with vehicle alone. Data were normalized to actin mRNA and to 1 for vehicle. Eight mice per group were studied with similar results. ANOVA with the Newman–Keuls multicomparison test was carried out. *, $P < 0.05$, $CD105^+$ MV versus $CD105^-$ MV. D, representative immunohistochemistry for MMP9 and MMP2 on lung sections obtained from mice treated for 5 days with 70 μg of $CD105^+$ MVs or $CD105^-$ MVs or with vehicle alone showing MMP9 staining of vessels and alveolar epithelial cells (arrows and inset) and MMP2 staining of vessels (inset) in $CD105^+$ MV–treated mice (original magnification: MMP9, ×200; MMP2, ×400; insets, ×620).

Moreover, miR-19b, miR-29c, and miR-151 were observed upregulated in renal carcinomas in comparison with normal renal tissue (48) and they were significantly enriched within miRNAs present in $CD105^+$ MVs.

It has been recently suggested that tumor-derived MVs may contribute to the formation of a premetastatic niche (37, 38). Herein, we showed that MVs derived from $CD105^+$ renal cancer stem cells, but not from $CD105^-$ tumor cells, were able to significantly enhance lung metastasis formation when injected prior to a renal tumor cell line. Indeed, $CD105^+$ MVs, but not $CD105^-$ MVs, significantly enhanced the expression of VEGFR1, VEGF, and MMP2 in CD146-sorted lung cells

Published OnlineFirst June 13, 2011; DOI: 10.1158/0008-5472.CAN-11-0241

containing endothelial cells and a small population of both leukocytes and MMP9 in the whole lung. Previous studies showed that these factors are involved in the generation of lung premetastatic niche (49, 50). Our results confirm that MVs create a receptive microenvironment to coordinate metastatic diffusion (37) and identify the specific contribution of MVs derived from cancer stem cells.

A recent study indicated that tumor stem cells not only initiate tumors but may also promote metastases in virtue of their peculiar content of tumorigenic miRNAs (46). MVs may transfer products of oncogenes to bystander cells, inducing changes in their phenotype (11). The result of the present study suggests that the RNA content of MVs plays a critical role, as the RNase treatment of MVs significantly inhibited the *in vitro* and in particular the *in vivo* biological effects of $CD105^+$ MVs. This suggests that the effects of $CD105^+$ MVs could be, at least in part, accounted for epigenetic changes induced by transfer of mRNAs and/or miRNAs.

In conclusion, the results of the present study suggest that, in renal cancer, the MVs that favor tumor growth and invasion were those that were derived from the cancer stem cells rather than from the whole tumor cell population. These MVs by enhancing tumor vascularization and by contributing to the establishment of a premetastatic niche may sustain an unfavorable outcome of the tumor.

Disclosure of Potential Conflicts of Interest

No potential conflicts of interest were disclosed.

Acknowledgments

The technical assistance of Federica Antico and Ada Castelli is gratefully acknowledged.

Grant Support

This study was supported by Associazione Italiana per la Ricerca sul Cancro (A.I.R.C.), project IG8912, by Italian Ministry of University and Research (MIUR) Prin08, and by Regione Piemonte, Project Oncoprot and Piattaforme Biotecnologiche, Pi-Stem project.

The costs of publication of this article were defrayed in part by the payment of page charges. This article must therefore be hereby marked *advertisement* in accordance with 18 U.S.C. Section 1734 solely to indicate this fact.

Received January 21, 2011; revised May 25, 2011; accepted May 31, 2011; published OnlineFirst June 12, 2011.

References

1. Ratajczak J, Wysoczynski M, Hayek F, Janowska-Wieczorek A, Ratajczak MZ. Membrane-derived microvesicles: important and underappreciated mediators of cell-to-cell communication. Leukemia 2006;20:1487–95.
2. Quesenberry PJ, Aliotta JM. The paradoxical dynamism of marrow stem cells: considerations of stem cells, niches, and microvesicles. Stem Cell Rev 2008;4:137–47.
3. Cocucci E, Racchetti G, Meldolesi J. Shedding microvesicles: artefacts no more. Trends Cell Biol 2008;19:43–51.
4. Muralidharan-Chari V, Clancy JW, Sedgwick A, D'Souza-Schorey C. Microvesicles: mediators of extracellular communication during cancer progression. J Cell Sci 2010;123:1603–11.
5. Van Doormaal FF, Kleinjan A, Di Nisio M, Büller HR, Nieuwland R. Cell-derived microvesicles and cancer. Neth J Med 2009;67:266–73.
6. Castellana D, Zobairi F, Martinez MC, Panaro MA, Mitolo V, Freyssinet JM, et al. Membrane microvesicles as actors in the establishment of a favorable prostatic tumoral niche: a role for activated fibroblasts and CX3CL1-CX3CR1 axis. Cancer Res 2009;69:785–93.
7. Ratajczak J, Miekus K, Kucia M, Zhang J, Reca R, Dvorak P, et al. Embryonic stem cell-derived microvesicles reprogram hematopoietic progenitors: evidence for horizontal transfer of mRNA and protein delivery. Leukemia 2006;20:847–56.
8. Deregibus MC, Cantaluppi V, Calogero R, Lo Iacono M, Tetta C, Biancone L, et al. Endothelial progenitor cell derived microvesicles activate an angiogenic program in endothelial cells by a horizontal transfer of mRNA. Blood 2007;110:2440–8.
9. Valadi H, Ekström K, Bossios A, Sjöstrand M, Lee JJ, Lötvall JO. Exosome-mediated transfer of mRNAs and microRNAs is a novel mechanism of genetic exchange between cells. Nat Cell Biol 2007;9:654–9.
10. Kosaka N, Iguchi H, Yoshioka Y, Takeshita F, Matsuki Y, Ochiya T. Secretory mechanisms and intercellular transfer of microRNAs in living cells. J Biol Chem 2010;285:17442–52.
11. Al-Nedawi K, Meehan B, Kerbel RS, Allison AC, Rak J. Endothelial expression of autocrine VEGF upon the uptake of tumor-derived microvesicles containing oncogenic EGFR. Proc Natl Acad Sci U S A 2009;106:3794–9.
12. Kosaka N, Iguchi H, Ochiya T. Circulating microRNA in body fluid: a new potential biomarker for cancer diagnosis and prognosis. Cancer Sci 2010;101:2087–92.
13. Reya T, Morrison SJ, Clarcke MF, Weissman IL. Stem cells, cancer, and cancer stem cells. Nature 2001;414:105–11.
14. Bussolati B, Bruno S, Grange C, Ferrando U, Camussi G. Identification of a tumor-initiating stem cell population in human renal carcinomas. FASEB J 2008;22:3696–705.
15. Quesenberry PJ, Dooner MS, Aliotta JM. Stem cell plasticity revisited: the continuum marrow model and phenotypic changes mediated by microvesicles. Exp Hematol 2010;38:581–92.
16. Bussolati B, Russo S, Deambrosis I, Cantaluppi V, Volpe A, Ferrando U, et al. Expression of CD154 on renal cell carcinomas and effect on cell proliferation, motility and platelet-activating factor synthesis. Int J Cancer 2002;100:654–61.
17. Bruno S, Grange C, Deregibus MC, Calogero RA, Saviozzi S, Collino F, et al. Mesenchymal stem cell-derived microvesicles protect against acute tubular injury. J Am Soc Nephrol 2009;20:1053–67.
18. Schmittgen TD, Lee EJ, Jiang J, Sarkar A, Yang L, Elton TS, et al. Real-time PCR quantification of precursor and mature microRNA. Methods 2008;44:31–8.
19. Mestdagh P, Van Vlierberghe P, De Weer A, Muth D, Westermann F, Speleman F, et al. A novel and universal method for microRNA RT-qPCR data normalization. Genome Biol 2009;10:R64.
20. Collino F, Deregibus MC, Bruno S, Sterpone L, Aghemo G, Viltono L, et al. Microvesicles derived from adult human bone marrow and tissue specific mesenchymal stem cells shuttle selected pattern of miRNAs. PLoS One 2010;5:e11803.
21. Fonsato V, Buttiglieri S, Deregibus MC, Bussolati B, Caselli E, Di Luca D, et al. PAX2 expression by HHV-8-infected endothelial cells induced a proangiogenic and proinvasive phenotype. Blood 2008;111:2806–15.
22. Bussolati B, Deambrosis I, Russo S, Deregibus MC, Camussi G. Altered angiogenesis and survival in human tumor-derived endothelial cells. FASEB J 2003;17:1159–61.
23. Yan M, Xu Q, Zhang P, Zhou XJ, Zhang ZY, Chen WT. BMC Correlation of NF-kappaB signal pathway with tumor metastasis of human head and neck squamous cell carcinoma. Cancer 2010;10:437–50.
24. Millimaggi D, Mari M, D'Ascenzo S, Carosa E, Jannini EA, Zucker S, et al. Tumor vesicle-associated CD147 modulates the angiogenic capability of endothelial cells. Neoplasia 2007;9:349–57.

Published OnlineFirst June 13, 2011; DOI: 10.1158/0008-5472.CAN-11-0241

25. Wysoczynski M, Ratajczak MZ. Lung cancer secreted microvesicles: underappreciated modulators of microenvironment in expanding tumors. Int J Cancer 2009;125:1595–603.
26. Hood JL, Pan H, Lanza GM, Wickline SA. Paracrine induction of endothelium by tumor exosomes. Lab Invest 2009;89:1317–28.
27. Baran J, Baj-Krzyworzeka M, Weglarczyk K, Szatanek R, Zembala M, Barbasz J, et al. Circulating tumour-derived microvesicles in plasma of gastric cancer patients. Cancer Immunol Immunother 2010;59: 841–50.
28. Taylor DD, Gercel-Taylor C. MicroRNA signatures of tumor-derived exosomes as diagnostic biomarkers of ovarian cancer. Gynecol Oncol 2008;110:13–21.
29. Friel AM, Corcoran C, Crown J, O'Driscoll L. Relevance of circulating tumor cells, extracellular nucleic acids, and exosomes in breast cancer. Breast Cancer Res Treat 2010;123:613–25.
30. Rabinowits G, Gerçel-Taylor C, Day JM, Taylor DD, Kloecker GH. Exosomal microRNA: a diagnostic marker for lung cancer. Clin Lung Cancer 2009;10:42–6.
31. Logozzi M, De Milito A, Lugini L, Borghi M, Calabrò L, Spada M, et al. High levels of exosomes expressing CD63 and caveolin-1 in plasma of melanoma patients. PLoS One 2009;4:e5219.
32. Skog J, Würdinger T, van Rijn S, Meijer DH, Gainche L, Sena-Esteves M, et al. Glioblastoma microvesicles transport RNA and proteins that promote tumour growth and provide diagnostic biomarkers. Nat Cell Biol 2008;10:1470–6.
33. Brase JC, Wuttig D, Kuner R, Sültmann H. Serum microRNAs as non-invasive biomarkers for cancer. Mol Cancer 2010;9:306–15.
34. Zen K, Zhang CY. Circulating MicroRNAs: a novel class of biomarkers to diagnose and monitor human cancers. Med Res Rev 2010 Nov 9. [Epub ahead of print].
35. Rosell R, Wei J, Taron M. Circulating microRNA signatures of tumor-derived exosomes for early diagnosis of non-small-cell lung cancer. Clin Lung Cancer 2009;10:8–9.
36. Baj-Krzyworzeka M, Szatanek R, Weglarczyk K, Baran J, Urbanowicz B, Brański P, et al. Tumour-derived microvesicles carry several surface determinants and mRNA of tumour cells and transfer some of these determinants to monocytes. Cancer Immunol Immunother 2006;55:808–18.
37. Jung T, Castellana D, Klingbeil P, Cuesta Hernández I, Vitacolonna M, Orlicky DJ, et al. CD44v6 dependence of premetastatic niche preparation by exosomes. Neoplasia 2009;11:1093–105.
38. McCready J, Sims JD, Chan D, Jay DG. Secretion of extracellular hsp90alpha via exosomes increases cancer cell motility: a role for plasminogen activation. BMC Cancer 2010;10:294.
39. Al-Nedawi K, Meehan B, Rak J. Microvesicles: messengers and mediators of tumor progression. Cell Cycle 2009;8:2014–8.
40. Aliotta JM, Pereira M, Johnson KW, de Paz N, Dooner MS, Puente N, et al. Microvesicle entry into marrow cells mediates tissue-specific changes in mRNA by direct delivery of mRNA and induction of transcription. Exp Hematol 2010;38:233–45.
41. Iorio MV, Visone R, Di Leva G, Donati V, Petrocca F, Casalini P, et al. MicroRNA signatures in human ovarian cancer. Cancer Res 2007;67: 8699–707.
42. Motoyama K, Inoue H, Takatsuno Y, Tanaka F, Mimori K, Uetake H, et al. Over- and under-expressed microRNAs in human colorectal cancer. Int J Oncol 2009;34:1069–75.
43. Brase JC, Johannes M, Schlomm T, Fälth M, Haese A, Steuber T, et al. Circulating miRNAs are correlated with tumor progression in prostate cancer. Int J Cancer 2011;128:608–16.
44. Mitchell PS, Parkin RK, Kroh EM, Fritz BR, Wyman SK, Pogosova-Agadjanyan EL, et al. Circulating microRNAs as stable blood-based markers for cancer detection. Proc Natl Acad Sci U S A 2008;105: 10513–8.
45. Gebeshuber CA, Zatloukal K, Martinez J. miR-29a suppresses tristetraprolin, which is a regulator of epithelial polarity and metastasis. EMBO Rep 2009;10:400–5.
46. Zhang X, Zhu W, Zhang J, Huo S, Zhou L, Gu Z, et al. MicroRNA-650 targets ING4 to promote gastric cancer tumorigenicity. Biochem Biophys Res Commun 2010;395:275–80.
47. Luedde T. MicroRNA-151 and its hosting gene FAK (focal adhesion kinase) regulate tumor cell migration and spreading of hepatocellular carcinoma. Hepatology 2010;52:1164–6.
48. Chow TF, Youssef YM, Lianidou E, Romaschin AD, Honey RJ, Stewart R, et al. Differential expression profiling of microRNAs and their potential involvement in renal cell carcinoma pathogenesis. Clin Biochem 2010;43:150–8.
49. Hiratsuka S, Nakamura K, Iwai S, Murakami M, Itoh T, Kijima H, et al. MMP9 induction by vascular endothelial growth factor receptor-1 is involved in lung-specific metastasis. Cancer Cell 2002;2:289–300.
50. Duda DG, Jain RK. Premetastatic lung "niche": is vascular endothelial growth factor receptor 1 activation required? Cancer Res 2010;70: 5670–3.

Published OnlineFirst June 13, 2011; DOI: 10.1158/0008-5472.CAN-11-0241

Cancer Research
The Journal of Cancer Research (1916–1930) | The American Journal of Cancer (1931–1940)

AACR American Association for Cancer Research

Microvesicles Released from Human Renal Cancer Stem Cells Stimulate Angiogenesis and Formation of Lung Premetastatic Niche

Cristina Grange, Marta Tapparo, Federica Collino, et al.

Cancer Res 2011;71:5346-5356. Published OnlineFirst June 13, 2011.